Journal of Materials Chemistry A

COMMUNICATION

View Article Online
View Journal | View Issue

Open Access Article. Published on 21 September 2015. Downloaded on 6/18/2026 12:49:49 PM.
This article is licensed under a Creative Commons Attribution 3.0 Unported Licence.

Cite this: J. Mater. Chem. A, 2015, 3, 20482

Received 14th August 2015
Accepted 20th September 2015

DOI: 10.1039/c5ta06394a

www.rsc.org/MaterialsA

Free-standing and binder-free highly N-doped carbon/sulfur cathodes with tailorable loading for high-areal-capacity lithium–sulfur batteries†

A. Schneider,[a] C. Suchomski,[b] H. Sommer,[ac] J. Janek*[ab] and T. Brezesinski*[a]

A facile hard-templating method has been developed to prepare highly N-doped carbon/sulfur cathodes with thickness < 200 μm and large areal mass loading (>2.5 mg_{sulfur} cm^{-2}). Lithium–sulfur batteries using this free-standing and binder-free hierarchical hybrid design exhibit good cycling performance, with stable areal capacities of 3.0 mA h cm^{-2}, owing to favorable properties of the carbon host.

With a theoretical specific capacity of 1675 mA h g^{-1}, sulfur has received much attention as an attractive cathode active material for high energy lithium–sulfur batteries.[1] The reader is referred to ref. 2 for the working principle of lithium–sulfur cells. However, a number of problems remain to be solved before they can be made commercially viable. For example, the specific properties of S_8 and Li_2S (*i.e.*, their electrically insulating nature and the solubility of lithium polysulfide species in organic electrolyte solvents) have a negative impact on the sulfur utilization,[1–3] and this in turn usually prevents high sulfur content and mass loading in the cathode—conditions that are necessary to be able to compete with high-performance lithium-ion batteries in general. While it is obvious that a high S/C ratio is required to achieve high specific capacities, it has often been overlooked that the electrolyte/sulfur (E/S) ratio strongly affects the cyclability as well, including sulfur utilization and capacity decay rate.[4] Unfortunately, this crucial information is rarely given, a major flaw that makes comparison of different cathode designs and materials virtually impossible and has led to conflicting results.

Over the past few years, various efforts have been made to address these problems by utilizing novel host materials, electrode structures and electrolytes.[5] Stable specific capacities of around 800 mA h g_{sulfur}^{-1} over 1000 cycles have been demonstrated for test cells with a low sulfur loading (<1.0 mg cm^{-2}).[6] In practice, low sulfur loading and high E/S ratio increase the longevity of lithium–sulfur batteries, but decrease the energy density considerably, thus leading to non-competitive cells.[7] To meet the requirements by automotive and other high energy density applications, sulfur loadings > 5.0 mg cm^{-2} in an electrolyte starved cathode (*i.e.*, with only a limited amount of electrolyte) are required.[7]

Besides paying attention to sulfur loading and E/S ratio, we focus, in this communication, on utilizing a highly conductive 3D carbon framework as the sulfur host. This cathode design not only ensures intimate contact between the sulfur particles and the carbon, but also allows for the possibility of saving some weight by reducing the amount of nonactive material.

In the following, we describe the preparation of free-standing and binder-free hierarchical N-doped carbon/sulfur cathodes for high-areal-capacity lithium–sulfur batteries through a facile hard-templating method using glass microfiber filter paper (Whatman Grade GF/A) and 1-ethyl-3-methylimidazolium dicyanamide (EMIM-DCA) as template and carbon precursor, respectively. In recent years, various synthetic approaches to free-standing sulfur composite cathodes with practical high loading have been reported.[8] Most of them have in common that they either incorporate carbon nanotubes or graphene. EMIM-DCA was chosen because this and other ionic liquids have been shown to be versatile precursors for the synthesis of heteroatom-containing carbonaceous materials with a high doping level and unique electronic properties.[9] In particular, nanoscale carbons with nitrogen dopants are of interest in technological applications, such as energy storage and electrocatalysis, to name only a few.[10] Moreover, they are capable of chemically confining sulfur species within the cathode architecture—thereby partly inhibiting the polysulfide shuttle effect and improving the long-term cycling performance.[11]

In short, for the synthesis, the microfiber filter was immersed in EMIM-DCA and full infiltration of the pore

[a]Battery and Electrochemistry Laboratory (BELLA), Institute of Nanotechnology, Karlsruhe Institute of Technology, Hermann-von-Helmholtz-Platz 1, 76344 Eggenstein-Leopoldshafen, Germany. E-mail: torsten.brezesinski@kit.edu

[b]Institute of Physical Chemistry, Justus-Liebig-University Giessen, Heinrich-Buff-Ring 58, 35392 Giessen, Germany. E-mail: juergen.janek@kit.de

[c]BASF SE, 67056 Ludwigshafen, Germany

† Electronic supplementary information (ESI) available. See DOI: 10.1039/c5ta06394a

This journal is © The Royal Society of Chemistry 2015

Open Access Article. Published on 21 September 2015. Downloaded on 6/18/2026 12:49:49 PM.
This article is licensed under a Creative Commons Attribution 3.0 Unported Licence.

network was achieved under vacuum. The soaked filter paper was then transferred to an oven and slowly heated under argon to 900 °C over the course of 4 h. Finally, the resulting N-doped carbon/glass composite was allowed to cool to room temperature. Infiltration and carbonization were repeated twice before removing the template by leaching with an aqueous solution of potassium hydroxide. Cathodes with sulfur loadings > 2.5 mg cm^{-2} were obtained by placing the appropriate amount of solid sulfur onto the carbon and applying heat (140–150 °C).

Fig. 1a shows a photograph of the original glass microfiber filter paper and N-doped carbon replica after removal of the template. We emphasize that the synthesized material is not only crack-free on the micrometer level, but also can be tailored in size and shape. The structure of the carbon at the top surface and in the interior was investigated using scanning electron microscopy (SEM). Fig. 1b–d show SEM images at different magnifications, which demonstrate that it can be templated by the glass microfiber structure (see also SEM images of the filter paper template in Fig. S1, ESI†). The thickness of the free-standing carbon—utilized as cathode host in the present work—is about 170 μm, and as is evident, it exhibits an interconnected pore network with porosity on multiple length scales. In addition, it can be seen that the carbon paper is not perfectly flat, but has some waviness, and the pores at the top surface are open.

The porosity was analyzed in more detail *via* nitrogen physisorption at 77 K (not shown) and mercury intrusion porosimetry. Fig. 2a shows both the cumulative pore volume and the relative pore volume derived from mercury intrusion porosimetry. These data corroborate the hierarchical nature of the pore

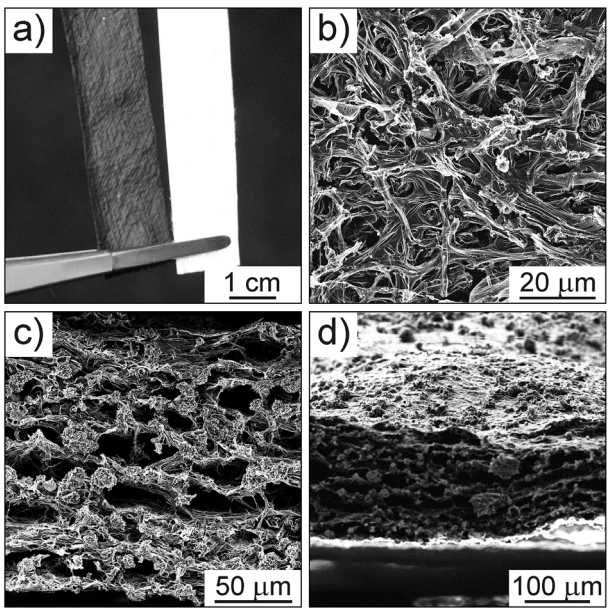

Fig. 1 (a) Photograph showing that free-standing, centimeter-sized carbon electrodes (black) can be fabricated by templating of glass microfiber filter paper (white). (b–d) Top view and cross-sectional SEM images at different magnifications of the (170 ± 10) μm-thick N-doped carbon host.

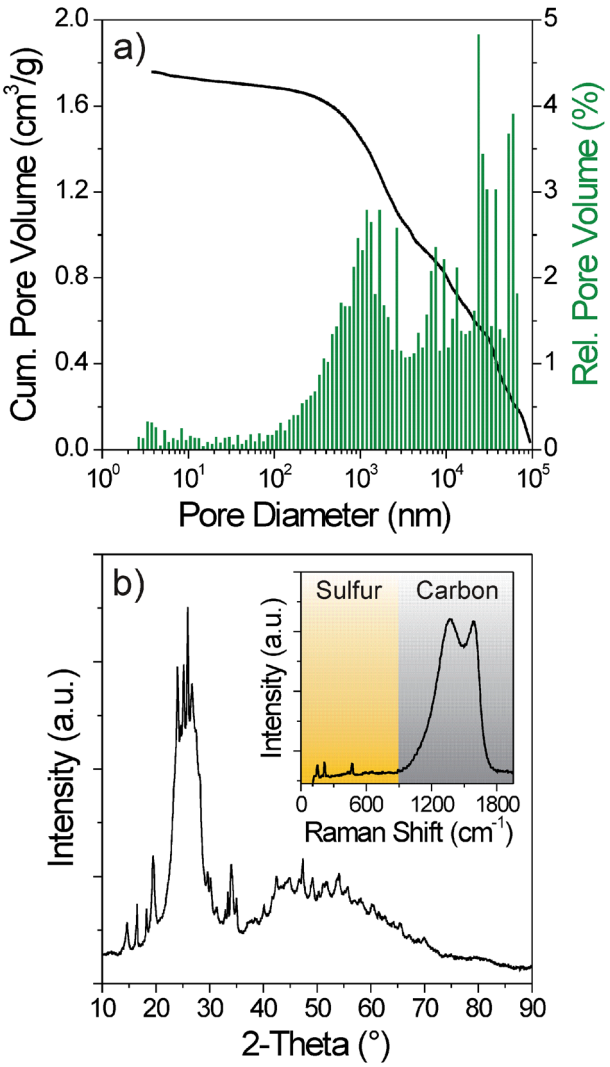

Fig. 2 (a) Cumulative and relative pore volume from mercury intrusion porosimetry showing that the carbon structure is hierarchical in nature. (b) XRD and Raman spectroscopy (inset) of the free-standing N-doped carbon after melt infiltration with 25 wt% sulfur.

structure. The size distribution is dominated by pores of diameter > 100 nm, in line with the microscopy results above. The total pore volume is 1.78 $cm^3\ g^{-1}$. BET analysis gives a specific surface area of about 80 $m^2\ g^{-1}$. The mesopore volume is in the range of 0.15 $cm^3\ g^{-1}$, *i.e.*, the sub-50 nm cavities contribute < 10% to the total pore volume.

The hard-templated carbon is found by elemental analysis to contain 12% N. High-temperature-treated carbonaceous materials with similar or even higher nitrogen content are scarce—the higher the carbonization temperature, the more nitrogen is eliminated.[9]

The crystallinity of the carbon/sulfur composite was investigated using X-ray diffraction (XRD) and Raman spectroscopy. The XRD pattern in Fig. 2b shows several broad reflections in the range of 2θ from 20° to 70°, which thus indicates that the N-doped carbon is turbostratic (partially graphitic). They result from the interlayer and intralayer scattering of the graphene

Open Access Article. Published on 21 September 2015. Downloaded on 6/18/2026 12:49:49 PM.
This article is licensed under a Creative Commons Attribution 3.0 Unported Licence.

sheets and are superimposed by reflections from nanocrystalline sulfur. The Raman spectrum in the inset of Fig. 2b also shows several bands. The D and G modes of carbon centered at 1370 and 1590 cm^{-1}, respectively, are found to be broad and strong. The in-plane correlation length or, in other words, the lateral extent of the graphene layers L_a can be determined from the ratio of peak heights using the Tuinstra and Koenig equation.[12] From this analysis we obtain a value of $L_a \approx 50$ Å, which is in the range observed for precursor-derived carbons and further corroborates the XRD results. The weak bands between 100 and 500 cm^{-1} are associated with bending and stretching modes of S_8.

Despite both the porosity and lack of significant crystallinity, the EMIM-DCA-derived carbon has a high electrical conductivity at room temperature (>1 S cm^{-1})—the nitrogen dopants increase the electronic conductivity through injection of additional electrons into the structure.[9,13] The carbon electrodes were embedded in an epoxy resin before determining the conductivity by four-probe measurement. The reason for this is that they are fragile and seem to have limited flexibility. Given that both S_8 and Li_2S are electrically insulating, the cathode host material (particularly in binder- and carbon additive-free electrodes) should be of high electronic conductivity and must have a certain level of void space to accommodate the volume expansion of sulfur during lithiation and to allow efficient transfer of electrons and good electrolyte penetration. The hierarchical carbon employed here fulfills these basic requirements.

The electrochemical testing was performed on coin-type cells consisting of hierarchical N-doped carbon/sulfur cathode and Li metal anode using 0.325 M LiTFSI and 0.675 M $LiNO_3$ in DOL/DME as electrolyte. The sulfur loading was varied between 2.5 and 8.5 mg cm^{-2} (equivalent to approx. 25–50 wt%) and the volume of electrolyte was set at 10 μL mg_{sulfur}^{-1}. The E/S ratio of about 10 : 1 by weight was chosen to compromise between specific capacity, coulombic efficiency and battery lifespan. The cycling performance was evaluated at C/20 after activation at a rate of C/50 (with 1C = 1673 mA g_{sulfur}^{-1}) in the potential range of 1.7–2.5 V with respect to Li/Li^+. The latter low-rate formation cycle improved the capacity retention on the subsequent cycles. We note that the cells show poor capacity retention at high rates, particularly when compared with structurally (and compositionally) tailored sulfur cathodes fabricated by a slurry coating method (see Fig. S2, ESI†). This, however, was somewhat expected, also because the electrodes were simply pressed onto an Al current collector for electrochemical cycling. Given that they have some waviness, any electrical contact issues during operation cannot be ruled out.

Representative voltage–capacity curves of the hierarchical N-doped carbon/sulfur cathode with 5 mg_{sulfur} cm^{-2} are shown in Fig. 3a. The profiles exhibit the typical plateaus of the lithium–sulfur battery system, corresponding to the successive conversion of S_8 to Li_2S and *vice versa*. As is seen, the sulfur utilization is only around 35% (550 mA h g_{sulfur}^{-1}) after the activation cycle with a discharge capacity of 1020 mA h g_{sulfur}^{-1}. Yet, the cells show stable cycling performance with areal capacities in excess of 2.7 mA h cm^{-2} (see Fig. 3b)—the specific capacity fades by only 0.03% per cycle after it has leveled off. This is an excellent result given that the volume of electrolyte used in these cells was comparably low. Furthermore, it is apparent that there is little increase in overpotential which helps to explain the good cyclability and stability at a rate of C/20. The coulombic efficiency is also higher than 99%, thus indicating reasonable reversibility of the free-standing and binder-free sulfur cathodes.

As previously mentioned, cathodes with lower and even higher areal mass loadings were also tested using the same cell configuration. From the inset of Fig. 3b, it can be seen that the sulfur utilization (or specific capacity per unit weight of sulfur) scales almost linearly with the loading, *i.e.*, only a certain fraction of sulfur is electrochemically active, while the rest acts as a kind of reservoir. Cathodes with 2.5 and 8.5 mg_{sulfur} cm^{-2} demonstrate sulfur utilizations of about 70% (1150 mA h

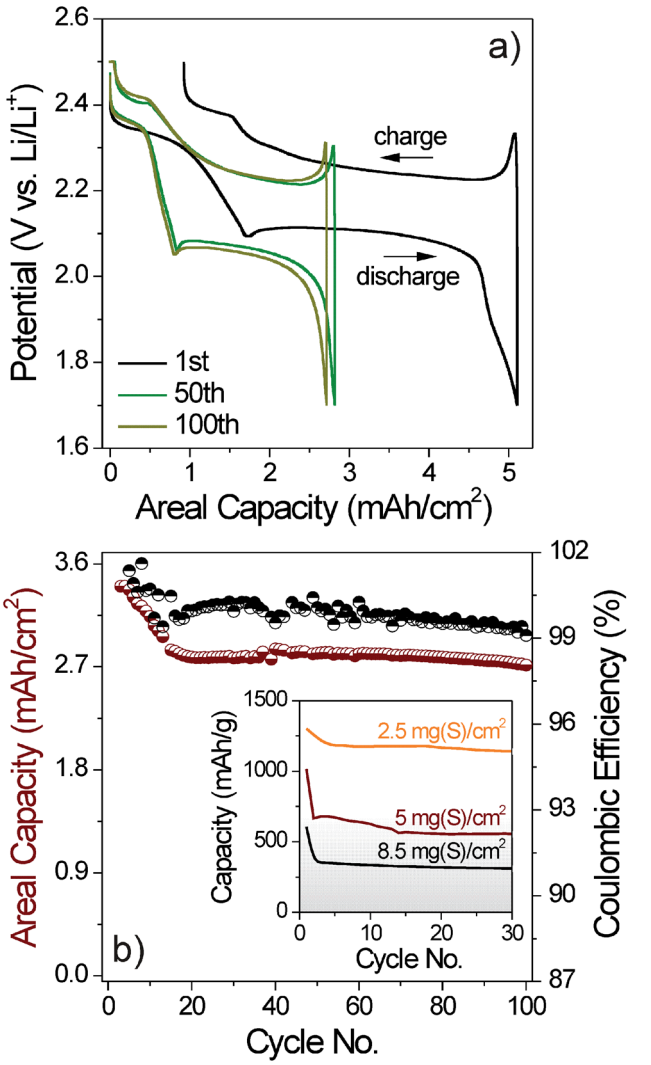

Fig. 3 Charge/discharge curves (a) and cycling performance (b) of the hierarchical N-doped carbon/sulfur cathode with 5 mg_{sulfur} cm^{-2}. After the first activation cycle at C/50 was completed, the rate was increased to C/20 for the subsequent cycles. Inset: specific capacity for different sulfur loadings.

This journal is © The Royal Society of Chemistry 2015

Open Access Article. Published on 21 September 2015. Downloaded on 6/18/2026 12:49:49 PM.
This article is licensed under a Creative Commons Attribution 3.0 Unported Licence.

g_{sulfur}^{-1}) and 20% (320 mA h g_{sulfur}^{-1}), respectively, at C/20. The sulfur utilization in low-loading cells is notable considering that the cathode structure has not been optimized yet. Overall, the fact that cells with different sulfur loadings and fixed E/S ratio deliver virtually the same areal capacity suggests that the number of surface sites available for adsorption of polysulfides and precipitation of S_8 and Li_2S is the limiting factor (rather than the loss of active material due to dissolution of lithium polysulfides into the electrolyte).

Finally, adsorption studies were undertaken to determine whether there are any specific interactions between the surface functional groups of the carbon and the lithium polysulfide species that may account for the excellent properties. To do so, 50 mg of N-doped carbon were placed into a vial containing 5 mL of a 1 mM solution of Li_2S_6 in tetrahydrofuran. After equilibration, the concentration of free polysulfide was determined by measuring the change in absorption at 415 nm through UV-Vis spectroscopy (see Fig. S3, ESI†). The EMIM-DCA-derived host material left 41% of polysulfide in solution or, in other words, it adsorbed 59% (adsorption capacity $\approx$ 0.012 $g_{polysulfide}$ g_{carbon}^{-1}). In addition, a reference experiment was conducted using hierarchical furfuryl alcohol-derived carbon paper prepared under identical conditions, except that the infiltration process was carried out at ambient pressure. This nitrogen-free carbon only adsorbed 24% (*i.e.*, about 2.5 times less), which provides evidence that the presence of nitrogen dopants not only alters the electronic properties, but also facilitates polysulfide binding through chemical interactions, in agreement with previous findings.[9–11] DFT studies have shown that lithium polysulfide species strongly interact with pyridinic and pyrrolic N sites. Overall, the combination of physical adsorption and chemical binding seems to be highly beneficial in improving the cycling performance.

Conclusions

In summary, a simple hard-templating method to obtain free-standing hierarchical N-doped carbon/sulfur cathodes—that can be tailored in terms of size and sulfur loading—for application in binder-free lithium–sulfur batteries is demonstrated. The synthesized carbon exhibits significant electronic conductivity and favorable adsorption properties due to the high nitrogen doping level, and is an attractive cathode host for sulfur; yet there is still room for improvement. Future work will be dedicated to optimizing the cathode design to increase sulfur utilization (particularly in high-loading cells) and rate capability, and to reducing the amount of electrolyte to achieve competitive energy densities. Finally, we note that similar performance results can be obtained for glass microfiber filter paper coated with a thin layer of the N-doped carbon. This allows for the intriguing possibility of reducing the overall costs.

Acknowledgements

This study is part of the projects being funded within the BASF International Network for Batteries and Electrochemistry.

Notes and references

1 P. G. Bruce, S. A. Freunberger, L. J. Hardwick and J.-M. Tarascon, *Nat. Mater.*, 2012, **11**, 19; B. Scrosati and J. Garche, *J. Power Sources*, 2010, **195**, 2419; X. Ji and L. Nazar, *J. Mater. Chem.*, 2010, **20**, 9821.

2 A. Manthiram, Y. Fu, S.-H. Chung, C. Zu and Y.-S. Su, *Chem. Rev.*, 2014, **114**, 11751; C. Barchasz, F. Molton, C. Duboc, J.-C. Lepretre, S. Patoux and F. Alloin, *Anal. Chem.*, 2012, **84**, 3973.

3 Y. V. Mikhaylik and J. R. Akridge, *J. Electrochem. Soc.*, 2004, **151**, A1969; M. R. Busche, P. Adelhelm, H. Sommer, H. Schneider, K. Leitner and J. Janek, *J. Power Sources*, 2014, **259**, 289.

4 M. Hagen, P. Fanz and J. Tübke, *J. Power Sources*, 2014, **264**, 30; S. Urbonaite and P. Novak, *J. Power Sources*, 2014, **249**, 497; A. Jozwiuk, H. Sommer, J. Janek and T. Brezesinski, *J. Power Sources*, 2015, **296**, 454.

5 X. Ji, K. T. Lee and L. Nazar, *Nat. Mater.*, 2009, **8**, 500; N. Jayaprakash, J. Shen, S. S. Moganty, A. Corona and L. A. Archer, *Angew. Chem., Int. Ed.*, 2011, **50**, 5904; C. D. Liang, N. J. Dudney and J. Y. Howe, *Chem. Mater.*, 2009, **21**, 4724; M. Barghamadi, A. S. Best, A. I. Bhatt, A. F. Hollenkamp, M. Musameh, R. J. Rees and T. Rüther, *Energy Environ. Sci.*, 2014, **7**, 3902; F. Lodi-Marzano, S. Leuthner, H. Sommer, T. Brezesinski and J. Janek, *Energy Technol.*, 2015, **3**, 830.

6 Z. W. Seh, W. Li, J. J. Cha, G. Zheng, Y. Yang, M. T. McDowell, P.-C. Hsu and Y. Cui, *Nat. Commun.*, 2013, **4**, 1331; M.-K. Song, Y. Zhang and E. J. Cairns, *Nano Lett.*, 2013, **13**, 5891.

7 D. Eroglu, K. R. Zavadil and K. G. Gallagher, *J. Electrochem. Soc.*, 2015, **162**, A982; M. Hagen, D. Hanselmann, K. Ahlbrecht, R. Maça, D. Gerber and J. Tübke, *Adv. Energy Mater.*, 2015, **5**, 1401986; D. Lv, J. Zheng, Q. Li, X. Xie, S. Ferrara, Z. Nie, L. B. Mehdi, N. D. Browning, J.-G. Zhang, G. L. Graff, J. Liu and J. Xiao, *Adv. Energy Mater.*, 2015, **5**, 1402290.

8 Z. Yuan, H.-J. Peng, J.-Q. Huang, X.-Y. Liu, D.-W. Wang, X.-B. Cheng and Q. Zhang, *Adv. Funct. Mater.*, 2014, **24**, 6105; G. Zhou, L. Li, C. Ma, S. Wang, Y. Shi, N. Koratkar, W. Ren, F. Li and H.-M. Cheng, *Nano Energy*, 2015, **11**, 356.

9 J. P. Paraknowitsch, J. Zhang, D. Su, A. Thomas and M. Antonietti, *Adv. Mater.*, 2010, **22**, 87; J. P. Paraknowitsch and A. Thomas, *Energy Environ. Sci.*, 2013, **6**, 2839; S. Zhang, M. S. Miran, A. Ikoma, K. Dokko and M. Watanabe, *J. Am. Chem. Soc.*, 2014, **136**, 1690.

10 Y. Zhai, Y. Dou, D. Zhao, P. F. Fulvio, R. T. Mayes and S. Dai, *Adv. Mater.*, 2011, **23**, 4828; W. Yang, T.-P. Fellinger and M. Antonietti, *J. Am. Chem. Soc.*, 2011, **133**, 206; H.-W. Liang, X. Zhuang, S. Brüller, X. Feng and K. Müllen, *Nat. Commun.*, 2014, **5**, 5973; A. Schneider, C. Weidmann, C. Suchomski, H. Sommer, J. Janek and T. Brezesinski, *Chem. Mater.*, 2015, **27**, 1674.

11 J. Song, T. Xu, M. L. Gordin, P. Zhu, D. Lv, Y.-B. Jiang, Y. Chen, Y. Duan and D. Wang, *Adv. Funct. Mater.*, 2014,

24, 1243; H.-J. Peng, T.-Z. Hou, Q. Zhang, J.-Q. Huang, X.-B. Cheng, M.-Q. Guo, Z. Yuan, L.-Y. He and F. Wei, *Adv. Mater. Interfaces*, 2014, **1**, 1400227; G. Zhou, E. Paek, G. S. Hwang and A. Manthiram, *Nat. Commun.*, 2015, **6**, 7760; F. Schipper, A. Vizintin, J. Ren, R. Dominko and T.-P. Fellinger, *ChemSusChem*, 2015, **8**, 3077.

12 F. Tuinstra and J. L. Koenig, *J. Chem. Phys.*, 1970, **53**, 1126.
13 H. J. Burch, J. A. Davies, E. Brown, L. Hao, S. Antoranz Contera, N. Grobert and J. F. Ryan, *Appl. Phys. Lett.*, 2006, **89**, 143110.

Open Access Article. Published on 21 September 2015. Downloaded on 6/18/2026 12:49:49 PM.
This article is licensed under a Creative Commons Attribution 3.0 Unported Licence.

This journal is © The Royal Society of Chemistry 2015